

General-lumps, -breathers, and hybrid solutions to (2+1)-dimensional generalized KDKK equation

Peisen Yuan(袁培森)[1], Jiaxin Qi(齐家馨)[3], Ziliang Li(李子良)[2], and Hongli An(安红利)[3,†]

Citation: Chin. Phys. B, 2021, 30 (**4**): 040503. DOI: 10.1088/1674-1056/abcf97
Journal homepage: http://cpb.iphy.ac.cn; http://iopscience.iop.org/cpb

What follows is a list of articles you may be interested in

Interaction properties of solitons for a couple of nonlinear evolution equations

Syed Tahir Raza Rizvi, Ishrat Bibi, Muhammad Younis, and Ahmet Bekir
Chin. Phys. B, 2021, 30 (**1**): 010502. DOI: 10.1088/1674-1056/abaed3

Localized characteristics of lump and interaction solutions to two extended Jimbo-Miwa equations

Yu-Hang Yin(尹宇航), Si-Jia Chen(陈思佳), and Xing Lü(吕兴)
Chin. Phys. B, 2020, 29 (**12**): 120502. DOI: 10.1088/1674-1056/aba9c4

Stable soliton propagation in a coupled (2+1) dimensional Ginzburg-Landau system

Li-Li Wang(王丽丽), Wen-Jun Liu(刘文军)
Chin. Phys. B, 2020, 29 (**7**): 070502. DOI: 10.1088/1674-1056/ab90ea

Lump, lumpoff and predictable rogue wave solutions to a dimensionally reduced Hirota bilinear equation

Haifeng Wang(王海峰), Yufeng Zhang(张玉峰)
Chin. Phys. B, 2020, 29 (**4**): 040501. DOI: 10.1088/1674-1056/ab75d7

Integrability of extended (2+1)-dimensional shallow water wave equation with Bell polynomials

Wang Yun-Hu, Chen Yong
Chin. Phys. B, 2013, 22 (**5**): 050509. DOI: 10.1088/1674-1056/22/5/050509

General M-lumps, T-breathers, and hybrid solutions to (2+1)-dimensional generalized KDKK equation*

Peisen Yuan(袁培森)[1], Jiaxin Qi(齐家馨)[3], Ziliang Li(李子良)[2], and Hongli An(安红利)[3,†]

[1] College of Artificial Intelligence, Nanjing Agricultural University, Nanjing 210095, China
[2] College of Oceanic and Atmospheric Sciences, Ocean University of China, Qingdao 266100, China
[3] College of Sciences, Nanjing Agricultural University, Nanjing 210095, China

(Received 20 October 2020; revised manuscript received 22 November 2020; accepted manuscript online 2 December 2020)

A special transformation is introduced and thereby leads to the N-soliton solution of the (2+1)-dimensional generalized Konopelchenko–Dubrovsky–Kaup–Kupershmidt (KDKK) equation. Then, by employing the long wave limit and imposing complex conjugate constraints to the related solitons, various localized interaction solutions are constructed, including the general M-lumps, T-breathers, and hybrid wave solutions. Dynamical behaviors of these solutions are investigated analytically and graphically. The solutions obtained are very helpful in studying the interaction phenomena of nonlinear localized waves. Therefore, we hope these results can provide some theoretical guidance to the experts in oceanography, atmospheric science, and weather forecasting.

Keywords: KDKK equation, Hirota bilinear method, high-order lump solution, T-breather solution, hybrid solution

PACS: 05.45.Yv, 02.30.Ik, 02.30.Jr **DOI:** 10.1088/1674-1056/abcf9f

1. Introduction

Exact solutions of nonlinear equations are very important. Not only because exact solutions can help us to obtain some useful physical information hidden in the model, but also because they can work as benchmarks to test and improve numerical algorithms, which may lead to some deeper applications.[1] Therefore, many experts have devoted themselves to constructing exact solutions of nonlinear equations and lots of effective methods have been proposed, including the inverse scattering theory, Bäcklund transformation, Darboux transformation, Wronskian and Casoratian techniques, variable separation approach, Hirota bilinear method, and so on.[2–17]

Among the above methods, the Hirota bilinear method is more popularly used to construct N-soliton solutions, breather and lump solutions of nonlinear equations due to its directness and simplicity. Solitons are stable waves. Breathers are partially localized on a background and periodic in a certain direction. While, lumps are localized in all directions in the space. Such lump solutions have been considered as perfect prototypes for explaining rogue wave dynamics in financial crisis, nonlinear optics, plasmas, oceanography, and Bose–Einstein condensates.[18–21] In recent years, the researches on the breather and lump solutions as well as their interactions have been a hot topic in physical areas and many results have been achieved. For example, Yue *et al.* derived N solitons, breather, and lump solutions of the nonlinear evolution equation.[22] Wang *et al.* obtained breather solutions of the Ito equation and analyzed their dynamics.[23] Liu *et al.* derived the breathers, lumps, and interaction solutions of the KP equation.[24] Zhang and Ma presented a class of lump solution of the (2+1)-dimensional SK equation via the generalized bilinear forms.[25] Zhang *et al.* gave the breather and lump solutions for the nonlocal KP equation,[26] and Yong *et al.*, based on symbolic computation, derived the lump solutions for the KPI equation.[27] Huang *et al.* investigated interaction solutions between kink soliton solutions and lumps of the generalized KP equation.[28] Wang and Zhang obtained some lump solutions for a reduced Hirota equation.[29] Ma and his coworkers computed lumps solutions for two combined fourth-order soliton equations[30,31] and nonlinear dispersive waves with higher-order dispersion relations.[32] And they showed that such lumps solutions had rich dynamical behaviors. Meanwhile, there is also some work on breather and lump solutions of other nonlinear equations.[33–38] However, we find that most work mentioned above only focuses on the low-order lump and breather solution. For the high-order solutions of breathers, lumps and their interactions, little work has been done due to the difficulty in selecting suitable parameters involved in N-solitons. However, such high-order breathers, lumps as well as the interaction solutions, compared with the corresponding 1-lump and 1-breather, have more importance and wide applications in real world. Therefore, it is worthy of studying the high-order breather, lump solutions, and interactions of nonlinear equations.

As analyzed above, in the present work we shall investi-

*Project supported by the National Natural Science Foundation of China (Grant No. 11775116) and the Jiangsu Qinglan High-Level Talent Project.
†Corresponding author. E-mail: hongli_an@njau.edu.cn
© 2021 Chinese Physical Society and IOP Publishing Ltd

gate higher-order breathers, lumps, and their interactions for the (2+1)-dimensional generalized KDKK equation, which takes a form of

$$u_t + h_1 u_{xxx} + h_2 u u_x + h_3 u_{xxxxx} + h_4 \int u_{yy}\,\mathrm{d}x + h_5 u_{xxy} + h_6 (u_x \int u_y\,\mathrm{d}x + u u_y) + h_7 (u_x u_{xx} + u u_{xxx}) + h_8 u^2 u_x = 0, \quad (1)$$

where $u = u(x,y,t)$ and h_i $(i = 1,2,\ldots,8)$ are real constants. This equation has been widely used in ocean dynamics, fluid mechanics, and plasma physics.[39–41] It is noted that under some special cases, the equation (1) corresponds to different physical models. For example, when $h_1 = h_2 = 0$, $h_3 = 1$, $h_4 = h_5 = -5$, $h_6 = -15$, $h_7 = 15$, and $h_8 = 45$, the equation turns to the (2+1)-dimensional B-type KP equation for the shallow water wave in fluids or electrostatic wave potential in plasmas.[42–45] While when $h_2 = 6h_1$, $h_6 = 4h_5$, and $h_3 = h_4 = h_7 = h_8 = 0$, the equation becomes to the (2+1)-dimensional breaking soliton equation for the interactions between a long wave propagating along the x axis and a Riemann wave along the y axis.[46,47] Therefore, it would be of great interest to study the general (2+1)-dimensional KDKK equation (1).

To conclude, motivated by the significance of the (2+1)-dimensional KDKK equation and wide applications of the lump and breather solutions, here we would like to investigate the general high-order lumps, breathers as well as their interactions. We hope that the results obtained can help experts to understand and study the propagations of nonlinear localized waves as well as other physical phenomena related. The outline of the paper is arranged as follows. In Section 2, by introducing a special transformation and coefficient constraint, the N-soliton solutions of the (2+1)-dimensional KDKK equation (1) are constructed. In Section 3, by using a long wave limit to the $2M$-solitons, the general M-lump solutions are derived and their dynamical behaviors are analyzed. In Section 4, by restricting the conjugate conditions to the parameters, the T-breather solutions are constructed. Numerical simulations are implemented, which show that the types of breathers and their propagation properties are determined by the parameters selected. In Section 5, some interaction solutions are given. Finally, a short conclusion is attached in the last section.

2. N-soliton solutions to the KDKK equation

In this section, our concern is with the construction of N-soliton solutions to the (2+1)-dimensional KDKK equation (1). For this purpose, a special transformation is introduced via

$$u = 12 h_1 h_2^{-1} (\ln f)_{xx}. \quad (2)$$

It is seen that under the coefficient constraints

$$2h_1 h_2^{-1} = 5h_3 h_7^{-1} = h_5 h_6^{-1} = h_7 h_8^{-1}. \quad (3)$$

Equation (1) can be readily written into the Hirota bilinear form

$$(D_x D_t + h_1 D_x^4 + h_3 D_x^6 + h_4 D_y^2 + h_5 D_x^3 D_y) f \cdot f = 0, \quad (4)$$

where D_x, D_y, and D_t are the bilinear derivative operators defined by

$$D_x^\alpha D_y^\beta D_t^\gamma (f \cdot g) = (\partial_x - \partial_{x'})^\alpha (\partial_y - \partial_{y'})^\beta \times (\partial_t - \partial_{t'})^\gamma f(x,y,t) g(x',y',t') \,|_{x'=x,y'=y,t'=t},$$

with α, β, and γ being nonnegative integers.

According to the Hirota bilinear direct method,[3] the N-soliton solutions to the (2+1)-dimensional KDKK equation (1) are derived

$$f = f_N = \sum_{\mu=0,1} \exp\left(\sum_{i=1}^{N} \mu_i \eta_i + \sum_{i<j}^{N} \mu_i \mu_j A_{ij} \right), \quad (5)$$

where

$$\eta_i = k_i (x + p_i y + \omega_i t) + \eta_i^0,$$
$$\omega_i = -h_3 k_i^4 - (h_1 + h_5 p_i) k_i^2 - h_4 p_i^2,$$

$$\mathrm{e}^{A_{ij}} = \frac{3h_1(k_i - k_j)^2 + 5h_3(k_i - k_j)^2(k_i^2 - k_i k_j + k_j^2) + h_5(k_i - k_j)(k_i p_j - k_j p_i + 2k_i p_i - 2k_j p_j) - h_4(p_i - p_j)^2}{3h_1(k_i + k_j)^2 + 5h_3(k_i + k_j)^2(k_i^2 + k_i k_j + k_j^2) + h_5(k_i + k_j)(k_i p_j + k_j p_i + 2k_i p_i + 2k_j p_j) - h_4(p_i - p_j)^2}, \quad (1 \le i, j \le N), \quad (6)$$

where k_i, p_i, ω_i, and η_i^0 are constants related to the amplitude and phase of the i-th soliton. While $\sum_{\mu=0,1}$ means a summation over all possible combinations of μ_i, $\mu_j = 0, 1$.

3. M-lump solutions to the KDKK equation

This section is focused on constructing the general M-lump solutions to the KDKK equation. In order to get the M-lump solutions, we set every $\eta_i^0 = \mathrm{i}\pi$ in Eq. (5). So that f_N can be rewritten into the following form:

$$f = f_N = \sum_{\mu=0,1} \prod_{i=1}^{N} (-1)^{\mu_i} \exp(\mu_i \xi_i) \prod_{i<j}^{N} \exp(\mu_i \mu_j A_{ij}), \quad (7)$$

with

$$\xi_i = k_i [x + p_i y - (h_1 k_i^2 + h_3 k_i^4 + h_4 p_i^2 + h_5 k_i^2 p_i) t]. \quad (8)$$

On taking a limit when $k_i \to 0$, we get

$$f = f_N = \sum_{\mu=0,1} \prod_{i=1}^{N} (-1)^{\mu_i} (1+\mu_i k_i \theta_i) \times \prod_{i<j}^{N} (1+\mu_i \mu_j k_i k_j B_{ij}) + O(k^{N+1}). \tag{9}$$

It can be easily seen that f_N has a symmetric feature on k_i, which renders it to have a factor of $\prod_{i=1}^{N} k_i$. For simplicity, we omit the factor $\prod_{i=1}^{N} k_i$ in f_N and still use f_N to record it. So the simplified f_N takes the following form:

$$f = f_N = \prod_{i=1}^{N} \theta_i + \frac{1}{2} \sum_{i,j}^{N} B_{ij} \prod_{l \neq i,j}^{N} \theta_l + \cdots + \frac{1}{M! 2^M} \sum_{i,j,\ldots,m,n}^{N} \overbrace{B_{ij} B_{kl} \ldots B_{mn}}^{M} \prod_{p \neq i,j,k,l,\ldots,m,n}^{N} \theta_p + \cdots, \tag{10}$$

where

$$\theta_i = x + p_i y - h_4 p_i^2 t, \quad B_{ij} = \frac{6(h_5 p_i + h_5 p_j + 2h_1)}{h_4 (p_i - p_j)^2}. \tag{11}$$

It is pointed out that the relation of Eq. (10) usually leads to a singular solution. However, if we require $p_{M+i} = p_i^*$ $(i = 1, 2, \ldots, M)$ with $N = 2M$ and $B_{ij} > 0$, we shall obtain a class of general M-lump solutions of the KDKK equation, which were claimed by Satsuma and Ablowitz in Ref. [48].

In the sequel, we shall apply the above procedure to construct the 1-lump solution of the KDKK equation (1). Therefore, we take $N = 2$, $M = 1$, and $\eta_1^0 = \eta_2^0 = \mathrm{i}\pi$. From Eq. (7), we have

$$f_2 = 1 - \mathrm{e}^{\xi_1} - \mathrm{e}^{\xi_2} + \mathrm{e}^{\xi_1 + \xi_2 + A_{12}}, \tag{12}$$

where

$$\xi_i = k_i [x + p_i y - (h_1 k_i^2 + h_3 k_i^4 + h_4 p_i^2 + h_5 k_i^2 p_i) t], \quad i = 1, 2. \tag{13}$$

When we apply the long wave limit of $k_i \to 0$ to f_2 and omit the constant factor $k_1 k_2$, we can get

$$f_2 = \theta_1 \theta_2 + B_{12}, \tag{14}$$

where θ_1, θ_2, and B_{ij} are defined by

$$\theta_i = x + p_i y - h_4 p_i^2 t, \quad (i = 1, 2), \quad B_{12} = \frac{6(h_5 p_1 + h_5 p_2 + 2h_1)}{h_4 (p_1 - p_2)^2}, \tag{15}$$

with p_i being complex constants. In order to obtain the lump solution, we set $p_2 = p_1^* = a - \mathrm{i}b$ in Eq. (15), so the expression of f_2 is reducible to

$$f_2 = \theta_1 \theta_1^* + B_{12} = (x' + a y')^2 + b^2 y'^2 \frac{3(a h_5 + h_1)}{b^2 h_4}, \tag{16}$$

where

$$x' = x + h_4 (a^2 + b^2) t, y' = y - 2a h_4 t. \tag{17}$$

When requiring the relation

$$3(a h_5 + h_1)/b^2 h_4 < 0$$

and substituting Eq. (16) into the following expression:

$$u = 12 h_1 h_2^{-1} (\ln f)_{xx},$$

we obtain the 1-lump solution

$$u = \frac{24 h_1 h_2^{-1} \left[b^2 y'^2 - (x' + a y')^2 - \frac{3(a h_5 + h_1)}{b^2 h_4} \right]}{\left[(x' + a y')^2 + b^2 y'^2 - \frac{3(a h_5 + h_1)}{b^2 h_4} \right]^2}. \tag{18}$$

The lump solution keeps moving along the line

$$y = -\frac{2ax}{a^2 + b^2}. \tag{19}$$

When $a \neq 0$, the trajectory along the path $[x(t), y(t)]$ is defined by

$$\begin{cases} x + a y + \Delta_1 t = \pm \sqrt{\Delta_3}, \\ b y + \Delta_2 t = 0, \end{cases} \tag{20}$$

with

$$\Delta_1 = (b^2 - a^2) h_4, \quad \Delta_2 = -2ab h_4, \quad \Delta_3 = -\frac{3(a h_5 + h_1)}{b^2 h_4}. \tag{21}$$

It can be checked that the solution (18) is a constant and keeps moving in a permanent lump status at the velocity of $v_x = -h_4 (a^2 + b^2)$ and $v_y = 2a h_4$. The 1-lump solution reaches its maximum

$$u_{\max} = \left| \frac{8 b^2 h_4 h_1}{(a h_5 + h_1) h_2} \right|.$$

However, when $(x, y) \to \infty$, the solution decays. Here we take the parameters $a = b = 1$ to exhibit the dynamical behaviors the 1-lump solution may posses. It can be seen from Fig. 1 that the 1-lump solution shows bright and dark solitons' behaviors. Moreover, such a solution keeps its velocity, shape, and amplitude unchanged during propagations.

When we take $N = 4$, $M = 2$ and $\eta_i^0 = \mathrm{i}\pi$ $(i = 1, 2, 3, 4)$. According to Eq. (10), the expression of f_4 is

$$f_4 = \theta_1 \theta_2 \theta_3 \theta_4 + B_{12} \theta_3 \theta_4 + B_{13} \theta_2 \theta_4 + B_{14} \theta_2 \theta_3 + B_{23} \theta_1 \theta_4 + B_{24} \theta_1 \theta_3 + B_{34} \theta_1 \theta_2 + B_{12} B_{34}$$

$$+B_{13}B_{24}+B_{14}B_{23}, \tag{22}$$

where

$$\theta_i = x+p_i y-h_4 p_i^2 t,$$
$$B_{ij} = \frac{6(h_5 p_i + h_5 p_j + 2h_1)}{h_4(p_i-p_j)^2}, \quad (1\le i<j\le 4). \tag{23}$$

When taking

$$p_{j+2} = p_j^* = a_j - \mathrm{i}b_j, \quad B_{ij}>0, \quad (j=1,2) \tag{24}$$

and inserting Eq. (22) into $u = 12h_1h_2^{-1}(\ln f)_{xx}$, we obtain the 2-lump solutions and their dynamical behaviors as shown in Fig. 2.

Analogously, if taking $N=6$, $M=3$, and $\eta_i^0 = \mathrm{i}\pi$ $(i=1,\ldots,6)$, one can write down the expression of f_6 from Eq. (10). When requiring $p_{i+3}=p_i^*$ $(i=1,2,3)$ and substituting them into f_6, we can obtain the 3-lump solution. Since the expression of the 3-lump solution is too lengthy, we just omit the details and only give the numerical simulations in Fig. 3. By comparing Fig. 3 with Fig. 2, we can find that both the 2- and 3-lumps will dramatically change their shapes and amplitudes in propagations and at a certain time there occur nonelastic collisions. Hence, it is believed that when these lump waves appear, some catastrophic weather or huge waves can happen in real world.

In the above discussion, we have shown that when $N=2M$ and taking the long wave limit to the $2M$-solitons, the general M-lump solutions will be generated. Such lump solutions are nonsingular and rationally localized. In the following, we shall demonstrate that when only adopting certain conjugation constrains to the parameters involved in $2T$-solitons, the general T-breather solutions will be constructed.

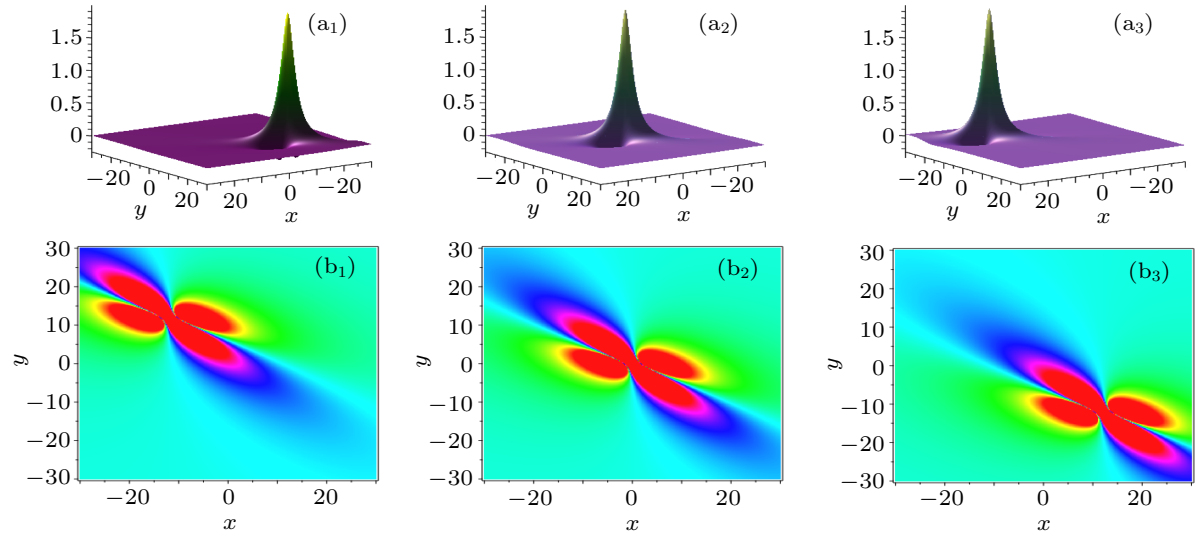


Fig. 1. Time evolutions of the 1-lump solution on *xoy* plane. The time is chosen as $t=3(i-2)$ for (a_i) and (b_i).

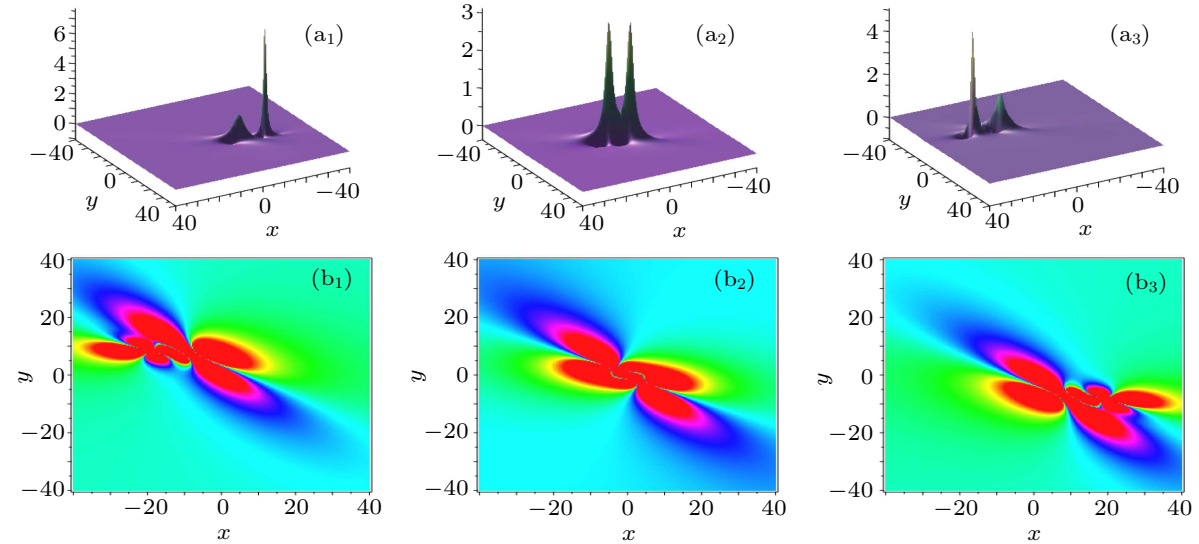


Fig. 2. Time evolutions of the 2-lump solution on *xoy* plane. The time is chosen as $t=2i-4$ for (a_i) and (b_i).

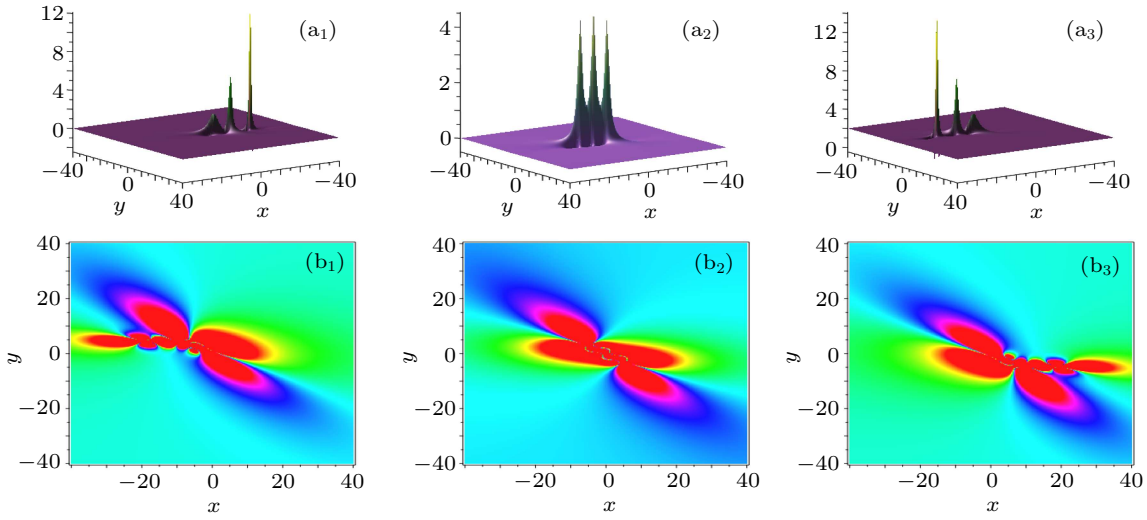


Fig. 3. Time evolutions of the 3-lump solution on xoy plane. The time is chosen as $t = i-2$ for (a_i) and (b_i).

4. T-breather solutions to the KDKK equation

In this section, we plan to construct high-order breather solutions to the KDKK equation. Hence, we introduce the conjugate constraints:

$$N = 2T, \quad k_{i+1} = k_i^*, \quad p_{i+1} = p_i^*,$$
$$\omega_{i+1} = \omega_i^*, \quad \eta_{i+1}^0 = \eta_i^{0^*}, \quad (i = 1,3,5,\ldots), \tag{25}$$

to the parameters involved in the $2T$-soliton solutions (5) and (6). For example, when $N = 2$, one can take the complex conjugate conditions as

$$k_2 = k_1^* = \alpha_1 - \mathrm{i}\gamma_1, \quad p_2 = p_1^* = \beta_1 - \mathrm{i}\delta_1,$$
$$\omega_2 = \omega_1^* = \rho_1 - \mathrm{i}\sigma_1, \quad \eta_2^0 = \eta_1^{0^*} = \eta_0. \tag{26}$$

On inserting the above relation into Eq. (5), we can obtain the first-order breather solution, which is expressed by

$$f = 1 + \mathrm{e}^{A_{12}} \exp(2\zeta_1) + 2\exp(\zeta_1)\cos(\xi_1), \tag{27}$$

with

$$\xi_1 = \gamma_1 x + (\alpha_1\delta_1 + \gamma_1\beta_1)y + (\alpha_1\sigma_1 + \gamma_1\rho_1)t, \quad \zeta_1 = \alpha_1 x + (\alpha_1\beta_1 - \gamma_1\delta_1)y + (\alpha_1\rho_1 - \gamma_1\sigma_1)t + \eta_0,$$
$$\mathrm{e}^{A_{12}} = \frac{-(5\alpha_1^2\gamma_1^2h_3 - 15\gamma_1^4h_3 + \alpha_1\delta_1\gamma_1h_5 + 3\beta_1\gamma_1^2h_5 - \delta_1^2h_4 + 3\gamma_1^2h_1)}{(15\alpha_1^4h_3 - 5\alpha_1^2\gamma_1^2h_3 + 3\alpha_1^2\beta_1h_5 - \alpha_1\delta_1\gamma_1h_5 + 3\alpha_1^2h_1 + \delta_1^2h_4)}. \tag{28}$$

Interestingly, we find that the first-order breather solution u given by Eq. (27) has three different types of dynamical behaviors according to the values of the parameters $\{k_i, p_i\}$ $(i = 1,2)$ selected. For simplicity, we take $\eta_i^0 = 0$ and the three types of structures are described as follows.

(i) When $\mathrm{Re}(k_1) = \alpha_1 \neq 0$ and $\alpha_1\beta_1 - \gamma_1\delta_1 = 0$, the first-order breather is shown to be periodic along the y axis, see Figs. 4(a_1) and 4(b_1).

(ii) When $\mathrm{Re}(k_1) = \alpha_1 = 0$ and $\alpha_1\beta_1 - \gamma_1\delta_1 \neq 0$, the first-order breather is shown to be periodic along the x axis, see Figs. 4(a_2) and 4(b_2).

(iii) When $\mathrm{Re}(k_1) = \alpha_1 \neq 0$ and $\alpha_1\beta_1 - \gamma_1\delta_1 \neq 0$, the first-order breather is shown to be periodic along the line $\alpha_1 x + (\alpha_1\beta_1 - \gamma_1\delta_1)y = 0$, see Figs. 4($a_3$) and 4($b_3$).

Similarly, when $N = 4$ and the parameters are chosen as

$$k_2 = k_1^* = \alpha_1 - \mathrm{i}\gamma_1, \quad p_2 = p_1^* = \beta_1 - \mathrm{i}\delta_1,$$
$$\omega_2 = \omega_1^* = \rho_1 - \mathrm{i}\sigma_1, \quad \eta_2^0 = \eta_1^{0^*},$$
$$k_4 = k_3^* = \alpha_2 - \mathrm{i}\gamma_2, \quad p_4 = p_3^* = \beta_2 - \mathrm{i}\delta_2,$$
$$\omega_4 = \omega_3^* = \rho_2 - \mathrm{i}\sigma_2, \quad \eta_4^0 = \eta_3^{0^*}, \tag{29}$$

we can obtain the second-order breather solutions. The propagations features and dynamical behaviors of these 2-breather solutions are detected in Fig. 5. It can be seen from these figures that the 2-breather solutions consist of two first-order breathers. Like the 1-breather solution, they also exhibit three types of dynamical behaviors due to the parameters $\{k_i, p_i\}$ $(i = 1,2,3,4)$ selected. For example, when k_i are all pure imaginary numbers and p_i are complex numbers, the 2-breather solutions are shown to be periodic along the x axis, see Figs. 5(a_1) and 5(b_1). When k_i are complex numbers and p_i are pure imaginary numbers, the 2-breather solutions turn to be periodic along the directions which are perpendicular to each other, see Figs. 5(a_2) and 5(b_2). While when k_1 is real number, p_1 is pure imaginary number and k_3, p_3 are complex numbers, the 2-breathers are shown be periodic along the directions intersecting each other at a certain angle, see Figs. 5(a_3) and (b_3).

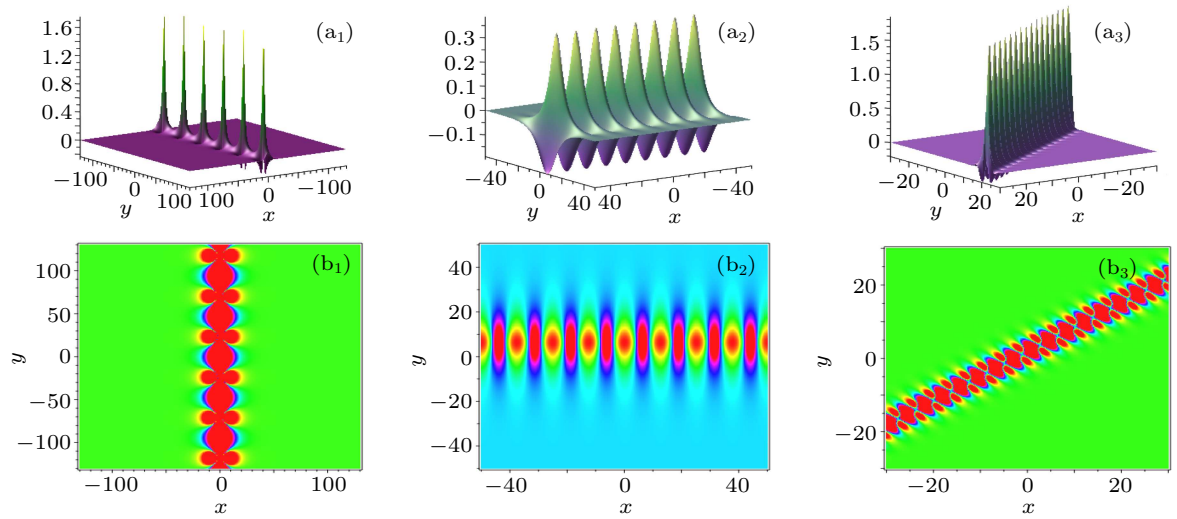


Fig. 4. Three types of behaviors of the first-order breather solution in *xoy* plane. The parameters are chosen as follows. In panels (a_1) and (b_1): $k_1 = 1/5$, $p_1 = (2/3)\mathrm{i}$; in panels (a_2) and (b_2): $k_1 = (1/2)\mathrm{i}$, $p_1 = (1/3)\mathrm{i}$; in panels (a_3) and (b_3): $k_1 = 1/2+\mathrm{i}, p_1 = 1/2+\mathrm{i}$.

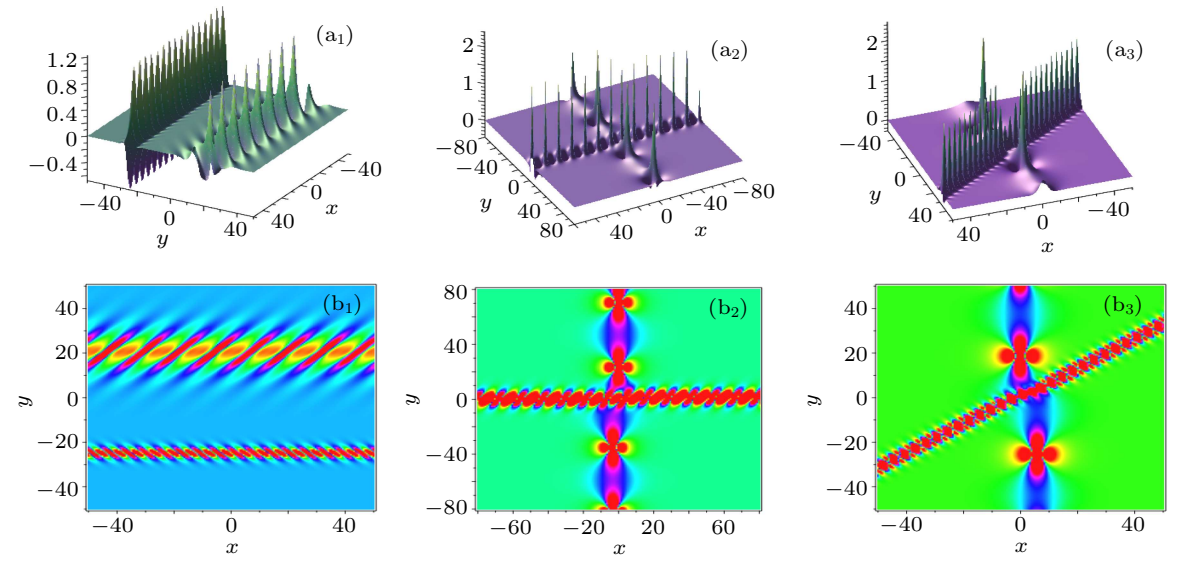


Fig. 5. Three types of behaviors of the 2-breather solution in *xoy* plane. The parameters are chosen as follows. In panels (a_1) and (b_1): $k_1 = \mathrm{i}$, $k_3 = (1/2)\mathrm{i}$, $p_1 = 1+\mathrm{i}$, $p_3 = -1+(1/2)\mathrm{i}$; in panels (a_2) and (b_2): $k_1 = (1/3)+\mathrm{i}$, $k_3 = -1+(1/2)\mathrm{i}$, $p_1 = (2/3)\mathrm{i}$, $p_3 = -(1/2)\mathrm{i}$; in panels (a_3) and (b_3): $k_1 = 1/4$, $k_3 = (1/2)+\mathrm{i}$, $p_1 = (2/3)\mathrm{i}$, $p_3 = (1/2)+\mathrm{i}$.

5. Hybrid wave solutions of the KDKK equation

5.1. Two kinds of hybrid solutions for $N = 3$

When $N = 3$, from Eq. (5), one can easily write down the expression of f_3, which is

$$\begin{aligned} f_3 \;=\; & 1+\mathrm{e}^{\eta_1}+\mathrm{e}^{\eta_2}+\mathrm{e}^{\eta_3}+\mathrm{e}^{\eta_1+\eta_2+A_{12}} \\ & +\mathrm{e}^{\eta_2+\eta_3+A_{23}}+\mathrm{e}^{\eta_1+\eta_3+A_{13}} \\ & +\mathrm{e}^{\eta_1+\eta_2+\eta_3+A_{12}+A_{13}+A_{23}}, \end{aligned} \tag{30}$$

where η_i, A_{ij} $(i,j = 1,2,3)$ are described in Eq. (6). In this subsection, two different techniques are applied to Eq. (30) and thereby two kinds of hybrid solutions are constructed. One is a kind of solution mixed by one lump and a stripe soliton via the long wave limit method established in Case 1. The other is a kind of solution combined by one breather and a strip soliton via the conjugate constraint method established in Case 2.

Case 1 An interaction solution between one lump and a stripe soliton

To construct a hybrid solution of one lump and a strip soliton, we set $\eta_i^0 = i\pi$ $(i = 1,2)$ and taking the limit as $k_1, k_2 \to 0$. Then the expression f_3 in Eq. (30) is reducible to

$$\begin{aligned} f \;=\; & \theta_1\theta_2 + B_{12} + (B_{12} + B_{13}B_{23} + B_{13}\theta_2 \\ & + B_{23}\theta_1 + \theta_1\theta_2)\exp(\eta_3), \end{aligned} \tag{31}$$

where

$$\begin{aligned} & \theta_1 = x + p_1 y - h_4 p_1^2 t, \quad \theta_2 = x + p_2 y - h_4 p_2^2 t, \\ & \eta_3 = k_3(x + p_3 y + \omega_3 t), \\ & \omega_3 = -h_3 k_3^4 - (h_1 + h_5 p_3)k_3^2 - h_4 p_3^2, \\ & B_{12} = \frac{6(h_5 p_1 + h_5 p_2 + 2h_1)}{h_4(p_1 - p_2)^2}, \quad B_{13} = B_{23} = 1. \end{aligned} \tag{32}$$

When setting $p_2 = p_1^* = a - b\mathrm{i}$ and requiring $(ah_5 + 2h_1)/h_4 b^2 < 0$, the expression u given via Eq. (31)

denotes a hybrid solution between one lump and a stripe soliton. Here we take $p_2 = p_1^* = 1 - \mathrm{i}$, $p_3 = -1.1$, and $k_3 = 1.2$ and dynamical behaviors of the solution given by Eq. (31) are simulated in Fig. 6. The time interval for the figures are 3 seconds. From the figures, we can see that: with the time evolution, the lump moves towards to the stripe soliton and then collides with the stripe solion at $t = 0$. After that, they keep moving forwards with their directions unchanged. However, their distances become farther and farther. What needs to point out is that no changes have happened to the velocity, energy and propagation directions during the collision. That's to say, the interactions between the lump and stripe soliton are elastic.

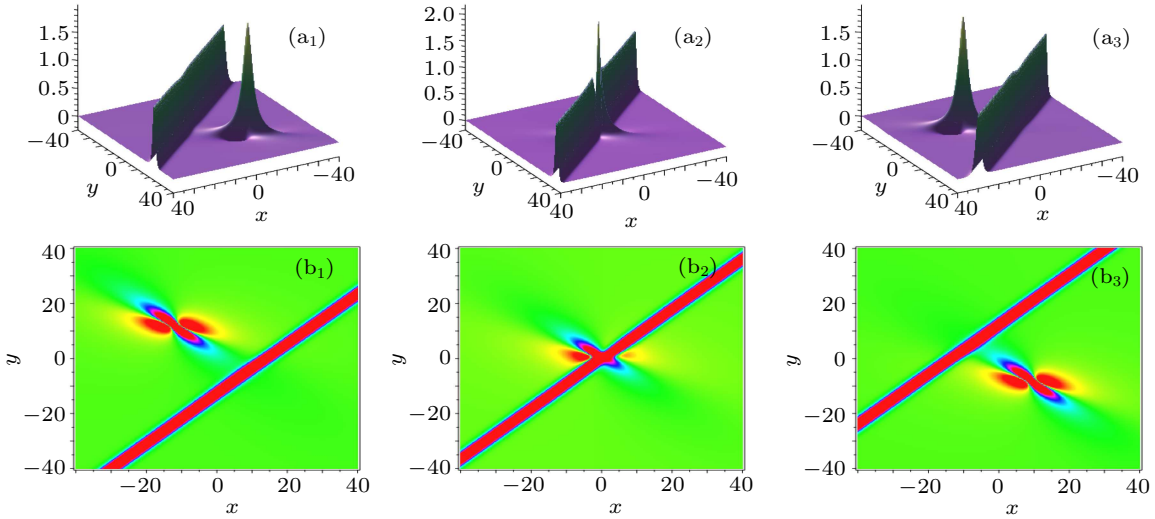


Fig. 6. Interaction behaviors of the hybrid solution given in Eq. (31). The time is chosen as $t = 3i - 6$ in panels (a_i) and (b_i).

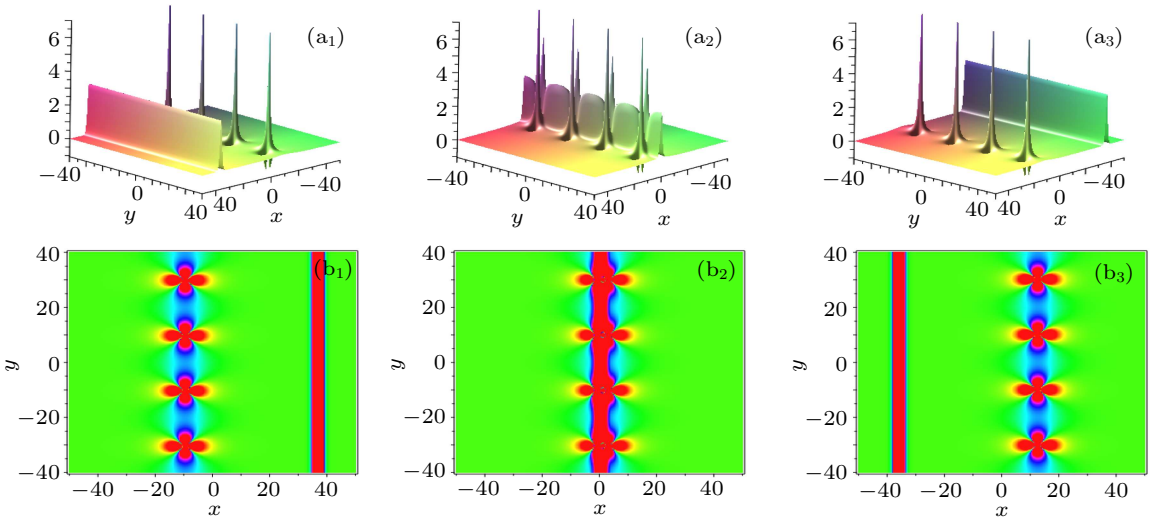


Fig. 7. Interaction behaviors of the hybrid solution given in Eq. (34). The parameters are chosen as $p_1 = (5/4)\mathrm{i}$, $k_1 = 1/4$, $k_3 = 2$, and $p_3 = 2$. The time is chosen as $t = 3i - 6$ for the figure (a_i) and (b_i).

Case 2 An interaction solution between one breather and a stripe soliton

To derive the hybrid solution of one breather and a stripe soliton, we set $\eta_i^0 = \eta_0$ $(i = 1, 2, 3)$ and introduce the following conjugate parameters:

$$k_2 = k_1^* = \alpha_1 - \mathrm{i}\gamma_1, \quad k_3 = \alpha_3,$$

$$p_2 = p_1^* = \beta_1 - \mathrm{i}\delta_1, \quad p_3 = \beta_3,$$

$$\omega_2 = \omega_1^* = \rho_1 - \mathrm{i}\sigma_1, \quad \omega_3 = \rho_3. \tag{33}$$

Substituting them into f_3 in Eq. (30), then we obtain

$$\begin{aligned} f \;=\; & 1 + 2\mathrm{e}^{\zeta_1}\cos(\xi_1) + \mathrm{e}^{\zeta_2} + A_{12}\mathrm{e}^{2\zeta_1} \\ & + 2\mathrm{e}^{\zeta_1+\zeta_2}[a\cos(\xi_1) - b\sin(\xi_1)] + A_{123}\mathrm{e}^{2\zeta_1+\zeta_2}, \end{aligned} \tag{34}$$

where

$$A_{12} = \frac{-(5\alpha_1^2\gamma_1^2 h_3 - 15\gamma_1^4 h_3 + \alpha_1\delta_1\gamma_1 h_5 + 3\beta_1\gamma_1^2 h_5 - \delta_1^2 h_4 + 3\gamma_1^2 h_1)}{(15\alpha_1^4 h_3 - 5\alpha_1^2\gamma_1^2 h_3 + 3\alpha_1^2\beta_1 h_5 - \alpha_1\delta_1\gamma_1 h_5 + 3\alpha_1^2 h_1 + \delta_1^2 h_4)},$$

$$\xi_1 = \gamma_1 x + (\gamma_1\beta_1 + \alpha_1\delta_1)y + (\gamma_1\rho_1 + \alpha_1\sigma_1)t, \quad \zeta_1 = \alpha_1 x + (\alpha_1\beta_1 - \gamma_1\delta_1)y + (\alpha_1\rho_1 - \gamma_1\sigma_1)t + \eta_0,$$
$$\zeta_2 = \alpha_3[x + \beta_3 y + \rho_3 t] + \eta_0, \quad A_{13} = A_{23}^*, \quad A_{123} = A_{12}A_{13}A_{23}, \quad a = \mathrm{Re}(A_{13}), \quad b = \mathrm{Im}(A_{13}). \tag{35}$$

The solution given via Eq. (34) represents a kind of hybrid solution between one breather and a stripe soliton. When we set the parameters as $p_1 = p_2^* = (5/4)\mathrm{i}$, $k_1 = k_2^* = 1/4$, $p_3 = 2$, and $k_3 = 2$, the dynamical behaviors of this hybrid solution are shown in Fig. 7. It can be seen from the figures that the breather in the hybrid solution is periodic along the direction that is perpendicular to the x axis on xoy plane. Also, one can find that the breather moves towards to the soliton and then collides with the soliton. After the collision, they keep moving with their directions and velocities unchanged. While, when we choose the parameters as $p_1 = 1/2 + 2\mathrm{i}$, $k_1 = (1/2) + \mathrm{i}$, $p_3 = 1.5$ and $k_3 = 1.2$, we find the breather in the hybrid solution is intersected to the stripe soliton at a certain angle, seen in Fig. 8.

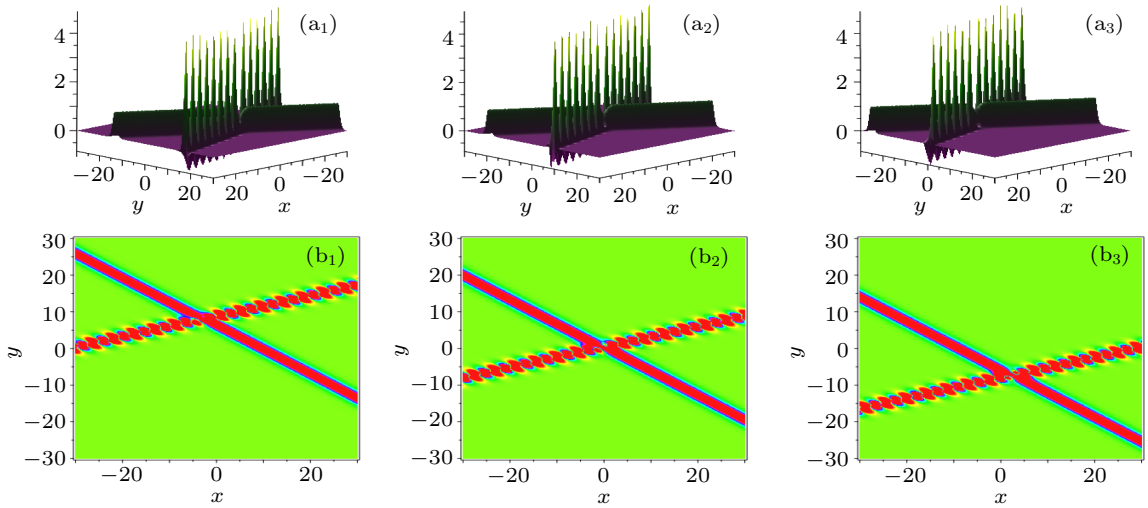


Fig. 8. Interaction behaviors of the hybrid solution given in Eq. (34). The parameters are chosen as $p_1 = 1/2 + 2\mathrm{i}$, $k_1 = 1/2 + \mathrm{i}$, $p_3 = 1.5$, and $k_3 = 1.2$. The time is chosen as $t = 3i - 6$ for the figure (a_i) and (b_i).

5.2. Three kinds of hybrid solutions for $N = 4$

When $N = 4$, from Eq. (5), one can get the expression of f_4. By taking long wave limit and restricting the conjugate conditions to f_4, three kinds of hybrid wave solutions can be obtained. Details are as follows.

Case 1 Two hybrid solutions between one lump and one breather or two bell-shaped solitons

Here, we take $\eta_1^0 = \eta_2^{0*} = \mathrm{i}\pi$ and $\chi_3^0 = \chi_4^0 = 0$. By taking the limit as $k_1, k_2 \to 0$, we obtain

$$\begin{aligned} f \;=\; & \theta_1\theta_2 + B_{12} + (\theta_1\theta_2 + B_{23}\theta_1 + B_{13}\theta_2 + B_{12} + B_{13}B_{23})e^{\eta_3} + (\theta_1\theta_2 + B_{24}\theta_1 + B_{14}\theta_2 + B_{12} + B_{14}B_{24})\,\mathrm{e}^{\eta_4} \\ & + B_{34}[\theta_1\theta_2 + (B_{23} + B_{24})\theta_1 + (B_{13} + B_{14})\theta_2 + B_{12} + (B_{13} + B_{14})(B_{23} + B_{24})]\,\mathrm{e}^{\eta_3+\eta_4}, \end{aligned} \tag{36}$$

where

$$\begin{aligned} & \theta_i = x + p_i y - h_4 p_i^2 t, \quad (i = 1, 2), \\ & \eta_j = k_j(x + p_j y + \omega_j t), \quad \omega_j = -h_3 k_j^4 - (h_1 + 5h_5 p_j)k_j^2 - h_4 p_j^2, \quad (j = 3, 4), \\ & B_{12} = \frac{6(h_5 p_1 + h_5 p_2 + 2h_1)}{h_4(p_1 - p_2)^2}, \quad B_{13} = B_{14} = B_{23} = B_{24} = 1, \\ & B_{34} = \frac{3h_1(k_3 - k_4)^2 + 5h_3(k_3 - k_4)^2(k_3^2 - k_3k_4 + k_4^2) + h_5(k_3 - k_4)(k_3p_4 - k_4p_3 + 2k_3p_3 - 2k_4p_4) - h_4(p_3 - p_4)^2}{3h_1(k_3 + k_4)^2 + 5h_3(k_3 + k_4)^2(k_3^2 + k_3k_4 + k_4^2) + h_5(k_3 + k_4)(k_3p_4 + k_4p_3 + 2k_3p_3 + 2k_4p_4) - h_4(p_3 - p_4)^2}. \end{aligned} \tag{37}$$

On inserting Eq. (36) into $u = 12h_1h_2^{-1}(\ln f)_{xx}$, two different kinds of interaction solutions can be obtained according to the values of the parameters k_3, k_4 and p_i $(i = 1, 2, 3, 4)$ selected.

(i) When $p_2 = p_1^*$, $p_4 = p_3^*$, and $k_4 = k_3^*$, the solution u given by Eq. (36) is a kind of hybrid solution combined by one lump and one breather. The dynamical behaviors are shown in Figs. 9 and 10. We can see from the figures that the breather is periodic along the x axis in Fig. 9 and it turns to be periodic along the y axis in Fig. 10.

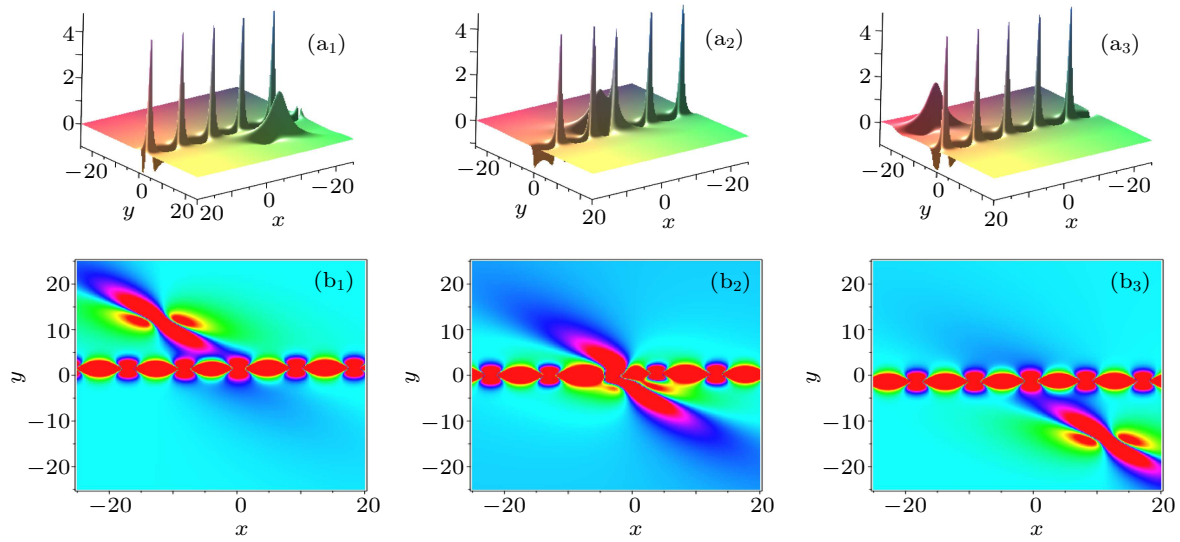


Fig. 9. Interactions of the hybrid solution between one lump and one breather. The parameters are chosen as $p_1 = p_2^* = 1+\mathrm{i}, k_3 = k_4^* = (7/10)\mathrm{i}$, and $p_3 = p_4^* = 2\mathrm{i}$. The time is chosen as $t = 3i-6$ for (a_i) and (b_i).

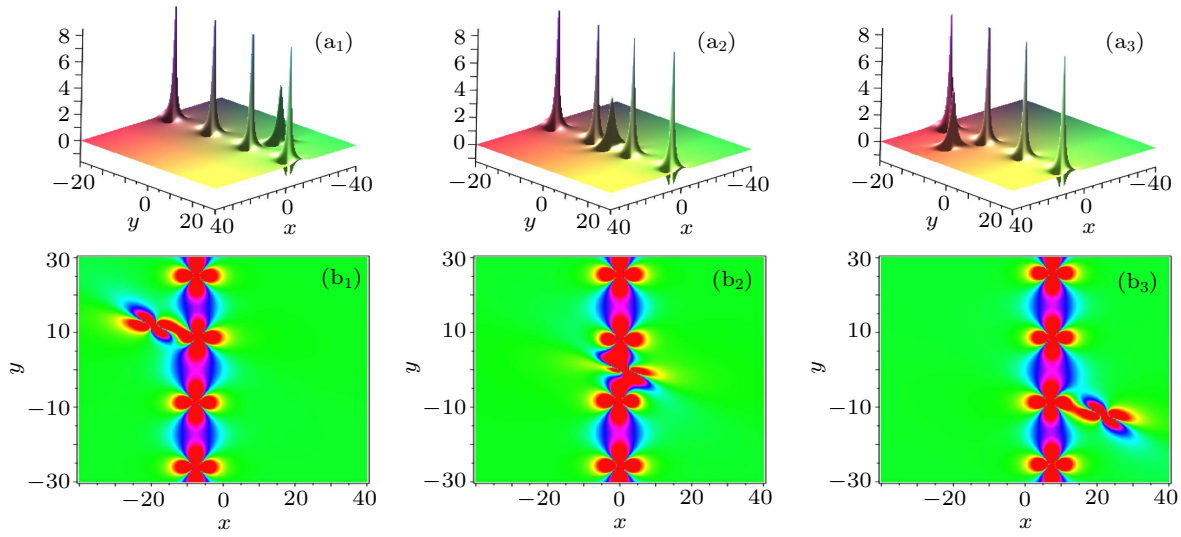


Fig. 10. Interactions of the hybrid solution between one lump and one breather. The parameters are chosen as $p_1 = p_2^* = 1+(3/2)\mathrm{i}, k_3 = k_4^* = 1/3$, and $p_3 = p_4^* = (11/10)\mathrm{i}$. The time is chosen as $t = 3i-6$ for (a_i) and (b_i).

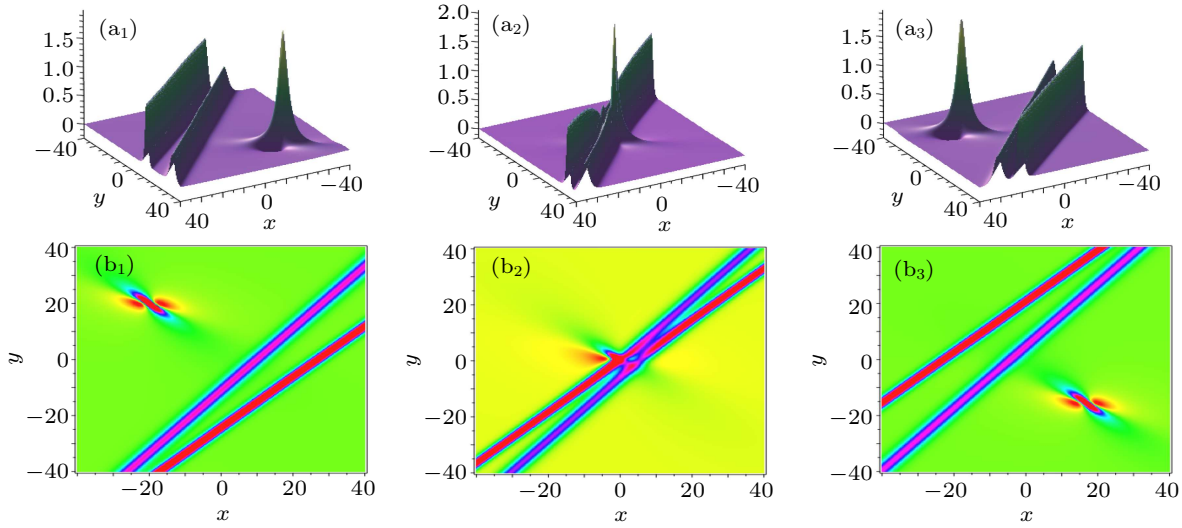


Fig. 11. Interactions of the hybrid solution between one lump and two bell-shaped solitons. The parameters are chosen as $p_1 = p_2^* = 1+\mathrm{i}$, $k_3 = 1.2$, $p_3 = -1.1$, $k_4 = 0.8$, $p_4 = -0.9$. The time is chosen as $t = 5i-10$ for (a_i) and (b_i).

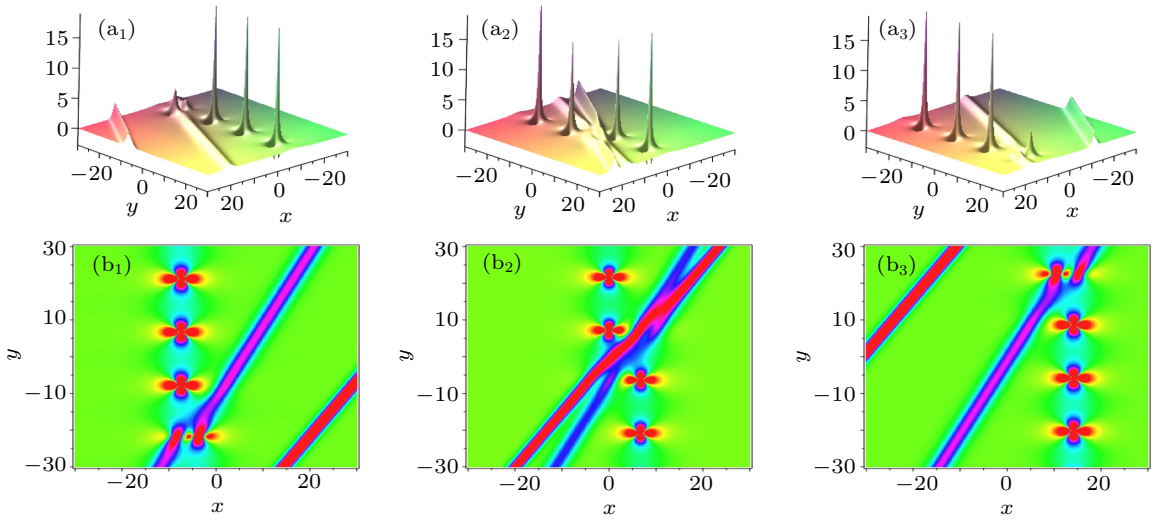


Fig. 12. Interaction behaviors between the breather and two bell-shaped solitons. The parameters are chosen by $p_1 = p_2^* = (13/12)\mathrm{i}$, $k_1 = k_2^* = 2/5$, $p_3 = -0.5$, $p_4 = -2/3$, $k_3 = 1$, and $k_4 = 1.8$. The time is chosen as $t = 3i - 6$ for (a_i) and (b_i).

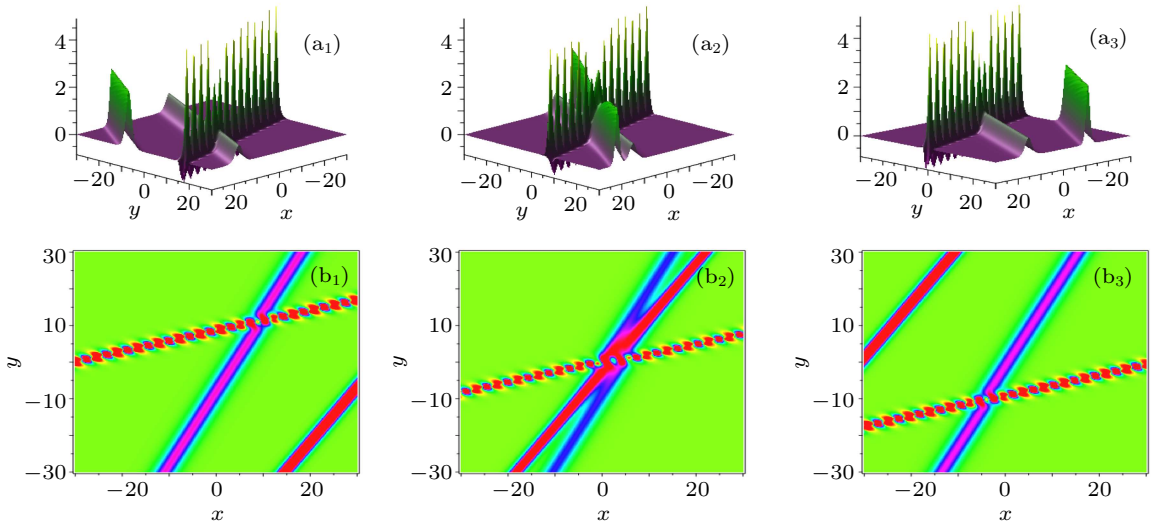


Fig. 13. Interaction behaviors between the breather and two bell-shaped solitons. The parameters are chosen by $p_1 = p_2^* = (1/2)+\mathrm{i}$, $k_1 = k_2^* = (1/2)+\mathrm{i}$, $p_3 = -0.5$, $p_4 = -2/3$, $k_3 = 1$, and $k_4 = 1.8$. The time is chosen as $t = 3i - 6$ for (a_i) and (b_i).

(ii) When $p_2 = p_1^*$ and p_3, p_4, k_3, and k_4 are real numbers, the solution u given by Eq. (36) denotes a kind of hybrid solution consisting of one lump and two bell-shaped solitons, whose dynamical behaviors are simulated in Fig. 11. Comparing with Fig. 6, one can see that, like the interactions between one lump and a bell-shaped soliton, the lump moves towards to the two bell-shaped solitons and then they collide with each other at $t = 0$. After that, they keep moving forwards without changing their directions but the distances between them become farther and farther.

Case 2 A hybrid solution between one breather and two bell-shaped solitons

Now, we set $\eta_i^0 = \eta_0$ $(i = 1,2,3)$ and introduce the following complex parameters

$$\begin{aligned} &k_2 = k_1^* = \alpha_1 - \mathrm{i}\gamma_1, \quad k_3 = \alpha_3, \quad k_4 = \alpha_4, \\ &p_2 = p_1^* = \beta_1 - \mathrm{i}\delta_1, \quad p_3 = \beta_3, \quad p_4 = \beta_4, \\ &\omega_2 = \omega_1^* = \rho_1 - \mathrm{i}\sigma_1, \quad \omega_3 = \rho_3, \quad \omega_4 = \rho_4. \end{aligned} \tag{38}$$

Substituting them into the expression of f_4 given by Eq. (5), we obtain an interaction solution between one breather and two bell-shaped solitons. When we take the parameters as $p_1 = p_2^* = (13/12)\mathrm{i}$, $k_1 = k_2^* = 2/5$, $p_3 = -0.5$, $p_4 = -2/3$, $k_3 = 1$, and $k_4 = 1.8$, and the breather in the hybrid solution is shown to be periodic along the y axis, seen in Fig. 12. While when we take $p_1 = p_2^* = 1/2+\mathrm{i}$, $k_1 = k_2^* = (1/2)+\mathrm{i}$, $p_3 = -0.5$, $p_4 = -2/3$, $k_3 = 1$, and $k_4 = 1.8$, the breather in the hybrid solution is shown to be periodic along the directions intersecting to xoy plane, seen in Fig. 13.

6. Conclusion

The investigation on exact solutions of the nonlinear equations is important and necessary because such solutions can better help us to understand the physical phenomena described by the model and lead to further applications. In this paper, we use the special transformation (2) to construct N-

soliton solutions of the (2+1)-dimensional generalized KDKK equation. By taking the long wave limit and the complex conjugation conditions to the N-solitons, we obtain the general M-lumps, T-breathers, and localized interaction solutions. Numerical simulations show that for the M-lumps, they usually collide with each other at certain time and their interactions are nonelastic (see Figs. 2 and 3). For the T-breathers and hybrid solutions, they have much richer dynamical behaviors than lumps, (see Figs. 4–13). Such behaviors are affected by the parameters selected. However, for the more complicated interaction solutions, due to the complexity in selecting the parameters, it is rather difficult to study their interactions, but they are worthy of deep investigation. In addition, how to use the solutions obtained to explain some physical phenomena, for example catastrophic weather and huge waves, is deserved our considerations. Meanwhile, whether the KDKK equation admits the multiple wave solutions is also an interesting questions deserved investigation. Based on the significance of the localized wave solutions and wide application of the KDKK equation, all these questions mentioned above will be further studied in the near future.

References

[1] Ablowitz M A and Clarkson P A 1991 *Soliton, Nonlinear Evolution Equations and Inverse Scatting* (NewYork: Cambridge University Press)
[2] Rogers C and Schief W K 2002 *Bäcklund and Darboux Transformations Geometry and Modern Applications in Soliton Theory* (NewYork: Cambridge University Press)
[3] Hirota R 2004 *The Direct Method in Soliton Theory* (NewYork: Cambridge University Press)
[4] Hu X B 1993 *J. Phys. A: Math. Gen.* **26** L465
[5] Cao C W, Wu Y T and Geng X G 1999 *J. Math. Phys.* **40** 3948
[6] Liu Q P and Manas M 2000 *Phys. Lett. B* **485** 293
[7] Ma W X and Fuchssteiner B 1996 *Int. J. Nonlinear Mech.* **31** 329
[8] Ma W X and You Y C 2005 *Trans. Amer. Math. Soc.* **357** 1753
[9] Lou S Y and Lu J Z 1996 *J. Phys. A: Math. Gen.* **29** 4209
[10] Fan E G 2000 *Phys. Lett. A* **277** 212
[11] Yan Z Y 2001 *Phys. Lett. A* **292** 100
[12] Chen Y and Wang Q 2006 *J. Appl. Math. Comput.* **177** 396
[13] Ma W X 2005 *Nonlinear Analysis* **63** e2461
[14] Trogdon T and Deconinck B 2013 *Appl. Math. Lett.* **26** 5
[15] Zhao P and Fan E G 2020 *Physica D* **402** 132213
[16] Tian S F 2017 *J. Diff. Equ.* **262** 506
[17] Wang D S, Guo B L and Wang X L 2019 *J. Diff. Equ.* **266** 5209
[18] Tajiri M and Arai T 1999 *Phys. Rev. E* **60** 2297
[19] Akhmediev N, Soto-Crespo J and Ankiewicz A 2009 *Phys. Rev. A* **80** 043818
[20] Kedziora D J, Ankiewicz A and Akhmediev N 2012 *Phys. Rev. E* **85** 066601
[21] He J S, Zhang H R, Wang L H and Fokas A S 2013 *Phys. Rev. E* **87** 052914
[22] Yue Y F, Huang L L and Chen Y 2018 *Comput. Math. Appl.* **75** 2538
[23] Wang X B, Tian S F, Qin C Y and Zhang T T 2017 *Appl. Math. Lett.* **68** 40
[24] Liu Y Q, Wen X Y and Wang D S 2019 *Comput. Math. Appl.* **78** 1
[25] Zhang H Q and Ma W X 2017 *Nonlinear Dyn.* **87** 2305
[26] Zhang X E, Chen Y and Zhang Y 2017 *Comput. Math. Appl.* **74** 2341
[27] Yong X L, Ma W X, Huang Y H and Liu Y 2018 *Comput. Math. Appl.* **75** 3414
[28] Huang L L, Yue Y F and Chen Y 2018 *Comput. Math. Appl.* **74** 831
[29] Wang H F and Zhang Y F 2020 *Chin. Phys. B* **29** 040501
[30] Ma W X, Zhang Y and Tang Y N 2020 *East Asian J. Appl. Math.* **10** 732
[31] Yang J Y, Ma W X and Khalique C M 2020 *Eur. Phys. J. Plus.* **135** 494
[32] Ma W X and Zhang L Q 2020 *Pramana-J. Phys.* **94** 43
[33] Ma W X 2015 *Phys. Lett. A* **379** 1975
[34] Lü X, Chen S T and Ma W X 2006 *Nonlinear Dyn.* **86** 523
[35] Wang J, An H L and Li B 2019 *Mod. Phys. Lett. B* **33** 1950262
[36] Yang J Y, Ma W X and Qin Z Y 2017 *Anal. Math. Phys.* **8** 427
[37] Yang J Y and Ma W X 2017 *Comput. Math. Appl.* **73** 220
[38] Wen X Y and Wang H T 2020 *Acta Phys. Sin.* **69** 010205 (in Chinese)
[39] Whitham G B 1974 *Linear and Nonlinear Waves* (New York: John Wiley & Sons)
[40] Kundu P K 1990 *Fluid Mechanics* (San Diego: Academic Press)
[41] Lamb H 1945 *Hydrodynamics* (Cambridge: Cambridge University Press)
[42] Lan Z, Gao Y, Yang J W, Su C Q and Wang Q 2016 *Mod. Phys. Lett. B* **30** 1650265
[43] Yang X, Fan R and Li B 2020 *Phys. Scr.* **95** 045213
[44] Peng W Q, Tian S F and Zhang T T 2018 *Phys. Lett. A* **382** 2701
[45] Feng L L, Tian S F, Wang X B and Zhang T T 2019 *Frontiers of Mathematics in China* **14** 631
[46] Lü X and Li J 2014 *Nonlinear Dyn.* **77** 135
[47] Xin X P, Liu X Q and Zhang L L 2010 *Appl. Math. Comput.* **215** 3669
[48] Satsuma J and Ablowitz M J 1979 *J. Math. Phys.* **20** 1496